

Orienting with Overhead Pins – An Exploratory Study Towards the Design of Part Feeders

Herbert F. Noriega, Kamal K. Gupta*, and Shahram Payandeh*

Abstract— This paper introduces aspects of an innovative method towards the development of a hybrid part orienter. Focusing on the principle of minimalism, we investigate the use of overhead pins of various classes over a slow moving conveyor to orient polygonal planar parts. We implement a simple planner that yields sequences of static passive pins to orient a given part from a random initial state to a final orientation set. We also encounter cases in which a single final orientation is not found, and thus, we introduce the use of a force/torque sensor (static active pin) to help distinguish between the possible orientations and be able to tell which results.

Limitations in orienting parts with overhead pins exist due to the complexity of the problem. Therefore, the purpose of our work is to serve as an initial study towards developing a part feeder that uses a new class of orienting devices, such as overhead pins.

Index Terms— overhead pins, part feeders, part orienting, force/torque sensor.

I. INTRODUCTION

Orienting parts refers to aligning a batch of parts to be assembled in a desired or unique configuration from an unknown initial configuration. The most common feeder used in manufacturing is the vibratory bowl feeder; however, the biggest drawback with this feeder is its lack of flexibility, wherein flexibility refers to "the ability to change a variety of parameters of the manufacturing process in response to business needs" [13]. Researchers have thus presented numerous designs to make part feeders more flexible and suitable to changing needs.

This paper introduces aspects of an innovative method towards the development of a hybrid part feeder. Hybrid refers to something that has two or more different types of components performing the same function. Here, we investigate the applicability and use of overhead pins of various classes, that is, pins with and without sensors, as well as static and moving pins, and combinations of these (see figure 1a), over a slow moving conveyor to orient polygonal planar parts. Our motivation for the use of pins is tied to the principle of minimalism, which refers to the simplest and minimal interaction between the orienting device and the part

to be oriented. Unlike fences that are used for the same orienting purpose, we do not rely on multiple point contact between the fence and the part, but instead we focus on a single point contact between the part and the pin at all times throughout the period of interaction as in figure 1b.

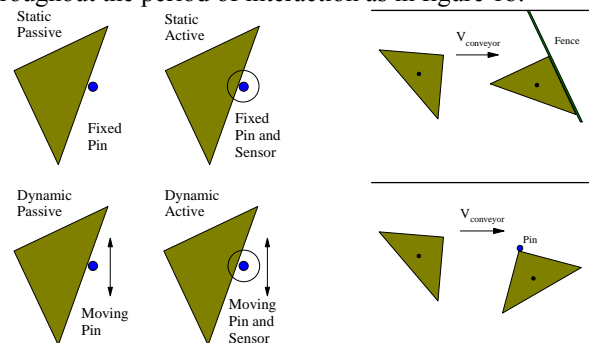


Figure 1 - a) Overhead pin classes and b) Fence contact vs. Pin Contact

Orienting with fences has the advantage that they guarantee that the part will rotate onto one of its natural resting edges as long as the fence is long enough for this motion to occur [8,9]. On the other hand, orienting with pins cannot take advantage of the part's stable edges in the same way. Thus, we must understand the behaviour of the part to be oriented as it comes into contact with a stationary pin (figure 1b), and consequently approximate the actual motion of the part. We return to the principle of minimum power [8,10] for this problem, and we make the assumption of a *constant and even pressure distribution* between the part and the surface it slides on. Hence, we approximate the motion of the workpiece by determining the instantaneous center of rotation (COR) given a set of conditions and assumptions.

The notion of orienting parts over a conveyor belt using fences was first introduced by Peshkin et al in [9]. Since, other work for orienting with fences include Akella et al using partial sensor information, with shape uncertainty, and innovatively reducing the problem to a single rotational fence in [1,2,3] respectively. Brokowski et al [6] added curved sections to the ends of fences to reduce uncertainty in the outcome and guarantee unique orientations. Also, Rusaw et al [11] incorporated a force/torque sensor to the problem of orienting with fences, while Salvarinov et al [12] manipulated parts using an active fence.

In addition, previous work using pins for part orienting include Zhang et al [15] in which pin sequences topple parts over a conveyor. On the other hand, Blind et al [5] used an array of retractable pins to manipulate the part on a vertical plate by capturing it. And more recently, Berretty et al [4] used pins as fingers to orient parts by inside-out pulling.

Manuscript received September 13, 2002. This work was supported in part by NSERC.

H. F. Noriega, K. K. Gupta and S. Payandeh are with the Experimental Robotics Laboratory, Simon Fraser University, Burnaby, BC V5A 1S6 Canada (e-mail: hfn@sfu.ca, kamal@cs.sfu.ca and shahram@cs.sfu.ca respectively).

*These authors appear in alphabetical order.

Finally, amongst other works in part orienting, Zhang et al [14] oriented parts by toppling through a series of steps.

Our work is an exploratory study along with [11,12,14] towards the future design and development of a more complete mechanics-based hybrid part feeder.

We implement a simple brute-force planner that yields sequences of static passive pins to orient the part from a random initial state to a final orientation set; thereby, providing a solution to the problem of part orienting using overhead pins as shown in figure 2 below.

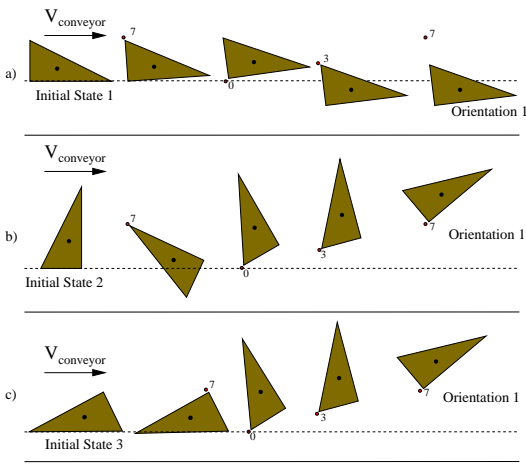


Figure 2 - Pin sequence used to orient an asymmetric triangular polygon from its three initial states to a final orientation. Pin labels are global labels indicating the chosen pins used to orient all initial states. The sequence must be the same in all cases.

The layout for the remainder of the paper is as follows: Section II examines the background theory and our approach used to model the motion of the polygonal part. Section III presents the part's motion simulation and experimental results, while section IV presents the planning results. Section V introduces the use of the force/torque (F/T) sensor and outlines the results obtained. Section VII summarizes the conclusion of the paper, and finally Section VIII outlines the future work to be done as a continuation to our study.

II. BACKGROUND AND THE MODELING APPROACH

This section presents some background material for the quasi-static motion simulation and outlines our approach used to model the motion of the polygonal part traveling on a slow moving conveyor and contacting a stationary overhead pin.

A. Quasi-static Motion Simulation

We refer to the previous studies by Peshkin and Sanderson [8] to understand the behaviour of a polygonal part against an overhead pin.

1) COR and Normal Pressure Distribution Assumption

The motion of a polygonal part can be characterized by its instantaneous center of rotation (COR), so that any infinitesimal motion of the part is a pure rotation $\delta\theta$ about its COR [6,8]. It was shown in [8] that this point and hence the motion of the part depends on the pressure distribution of the workpiece, which is generally unknown. Consequently, they introduced the COR locus, the area containing all the possible CORs given all possible pressure distributions, where its tip (r_{tip}), represents the point of slowest possible rotation for a

given polygon regardless of the pressure distribution. The r_{tip} of the locus has therefore been frequently used for the purpose of orienting with fences [1,2,3,6,9,11]. Using the locus tip it is possible to determine the minimum length of a fence that guarantees a given part comes to rest on one of its stable edges along the fence.

Unfortunately, we cannot take advantage of the slowest rotation when orienting with pins. Parts turning about CORs in the rest of the locus other than the tip of the locus rotate more and translate less than the slowest turning parts rotating about the r_{tip} [6]. Thus, orienting with pins requires that we approximate the motion of the part dependent on the instantaneous COR somewhere within the locus.

In our work, for the purpose of exploring the behaviour of planar parts with constant thickness and relatively smooth surfaces for part orienting, we find the instantaneous CORs for a given part geometry making the following assumption: *the planar polygons in our study have a constant and even pressure distribution over their entire area.*

Considering contact friction between the pin and the part, let μ_c be the contact friction coefficient. When $\mu_c > 0$ two modes of behaviour exist: *sticking* and *slipping*, and the applied force lies anywhere within the friction cone including its limits, where the cone's half angle ν is $\nu = \tan^{-1}\mu_c$. We utilize the findings in [8] to approximate the instantaneous CORs with friction at the point of contact assuming that μ_c is known and constant.

Subsequently, using these assumptions we resort to the notion of minimum power mechanics to solve for the instantaneous CORs that dictate the part's motion.

2) Minimum Power Mechanics

The minimum power principle presents the idea that the motion of the part, that is, the motion the part "chooses" to undergo, corresponds to that for which the energy dissipated to sliding friction (μ_k) is minimized [8]. This principle holds true only for the quasi-static approximation along with the simplest model of friction: Coulomb friction [10]. The total energy E_r lost to friction with the surface due to the rotation $\delta\theta$ as modified from [8] is:

$$E_r = \frac{\xi x \mu_s \sin \alpha}{\bar{\alpha} \cdot (\bar{c} - \bar{r})} P_w \iint_A \sqrt{(w_x - r_x)^2 + (w_y - r_y)^2} dw_y dw_x \quad (1)$$

We are interested in the location of the vector \bar{r} that minimizes this equation. Where w_x and w_y are the coordinates of a point in the area of a given polygon, and P_w is the term representing the constant even pressure distribution as per the stated assumption. Figure 3 illustrates the minimization process of E_r and the resulting instantaneous COR. We use the r_{tip} coordinates as the initial guess for the minimization function, and the scattered dots in figure 3 are the iterations' results towards finding the point of minimum energy E_r representing the instantaneous COR. Note the distinct location of the minimal energy COR and the COR locus tip.

We choose to integrate over the area A of the polygon rather than the area of the disc enclosing it [8]. Thus, we attempt to find a more representative instantaneous COR for the given polygon's geometry under the stated assumptions. Due to the

complexity of this integration, we explore FEA methods [7] to transform the general triangular polygon into a standardized rectangular polygon; thus, simplifying the calculations.

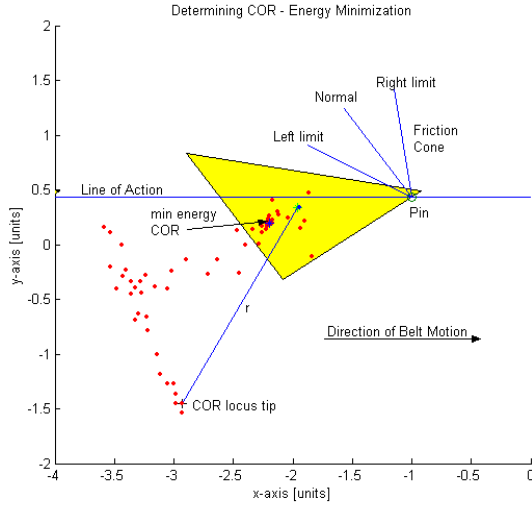


Figure 3 – Determining instantaneous COR using minimum power mechanics: starting with the COR locus tip, the minimization function finds a new instantaneous COR.

B. Configuration Maps

Configuration maps were first introduced in [9]. They encapsulate the physics of an operation such as a part contacting an overhead pin. Figure 4 illustrates a typical configuration map. The horizontal axis gives the initial orientation θ_i of the part prior to contact with the pin, while the vertical axis gives the final orientation θ_f after contacting the pin, rotating and sliding about it until losing contact.

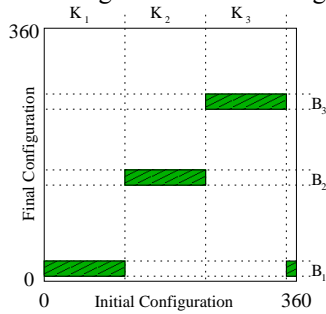


Figure 4 - Typical configuration map

Following the notation introduced in [9], the resulting map is composed of rectangular bands with ranges given by B_j ($j=1,2,3,\dots$) bounding the sets of final orientations and K_j bounding the sets of initial orientations. The bands in this map indicate the uncertain variation in rotation of a part due to the unknown pressure distributions.

In our case, the final orientations of a given polygon after contacting a stationary overhead pin, result from the relation:

$$\theta_f = f(\theta_i, d, \mu_c, P_w) \quad (2)$$

Where μ_c and P_w are assumed to be known constants and d is the contact parameter discussed in the next section. This relation implies a 1:1 mapping from initial to final orientation. But, given the uncertainty resulting from our assumptions, we group the adjacent common θ_f values using a set threshold

value T as follows:

$$|\theta_{f_{j+1}} - \theta_{f_j}| \leq T \quad (3)$$

These groups are then bounded by their maximum and minimum values and the result are intervals B_j along the θ_f axis as in the typical configuration map. For each group, the band interval is defined as follows:

$$B_j = [\min, \max) \{ \theta_f \in \text{group} \} \quad (4)$$

And the corresponding kernel interval K_j is defined as:

$$K_j = [\min, \max) \{ \theta_i \mid \alpha = f(\theta_i, d, \mu_c, P_w) \forall \alpha \in B_j \} \quad (5)$$

Of importance are also the center of mass (COM) intervals that result due to the variation in final orientations θ_f in the corresponding B_j .

$$COM_j = [\min, \max) \{ COM \mid \theta_f \Rightarrow COM \forall \theta_f \in B_j \} \quad (6)$$

These intervals are then used in the planning process.

C. Contact Parameter

Orienting with pins requires that we know the position of the polygon's COM and its perpendicular distance from the pin prior to contact with it. This perpendicular y -distance (see figure 5a) from the COM to the pin is referred to as the contact parameter (d). This contact parameter along with the part's initial orientation θ_i , μ_c and P_w determines the motion of the part when contacting an overhead pin as in expression (2).

We construct configuration maps for selected values of d to be used in the planning phase of our work. For simplicity, we label the contact parameter d as decimal fractions varying within $[0.1, 0.9]$ and $[-0.1, -0.9]$ of the geometric parameter a , where $a = \max(r_v)$, and r_v represents the part's radii measured from the part's COM to the part's vertices as shown in figure 5a. We use a as the geometric reference parameter because it represents the distance between the COM and the furthest point on the part.

Positive values of d correspond to pins located "above" the COM and negative values correspond to pins "below" as in figure 5b. The true perpendicular distance between the COM and the pin is the product da and it is geometry dependent.

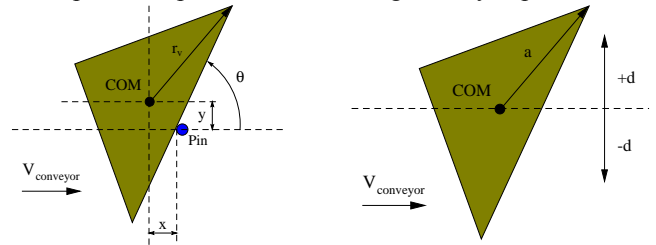


Figure 5 – a) Pin and COM distance. b) Positive and negative d .

D. Planning

The goal of planning is to find a sequence of pins that will orient a given part from a random initial state to a final orientation set. Planning with configuration maps was introduced in [9], where series of interactions are mapped by combining the maps corresponding to each individual action.

1) Complications due to the Contact Parameter

Unlike orienting with fences in which all initial unknown orientations are reduced to a set of natural resting states on the

first fence, orienting with pins does not offer that guarantee. Without a prior approximation of the distance between the COM and the pin it is nearly impossible to determine which contact parameters and corresponding configuration maps to use in the planning process. For this reason we reduce the initial uncertainty resulting from the unknown COM position. We decide on using the natural resting states of the given part as shown in figure 6 as the initial states from a common starting point. If necessary these states can be attained by using a curved fence as designed by Brokowski et al in [6].

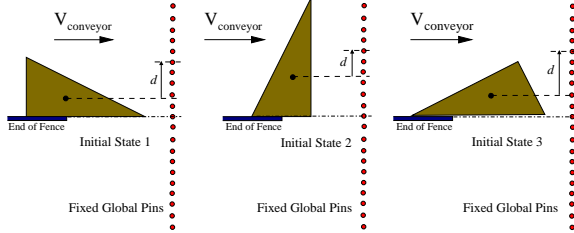


Figure 6 - Initial states for given triangular polygon and fixed global pins

2) The Search Tree – "Fixed Pins" Method

Due to varying COM positioning in the initial states of the given polygon as illustrated in figure 6, we cannot combine these without introducing a large amount of error in approximating a common reference line for the contact parameters and adapt the search method used in [9] and [11]. Instead, we opt on a breadth search method we refer to as the "fixed pins" method. This method requires two main issues:

- All pins to be used be positioned in global locations and hence be common to all initial states, see figure 6.
- A separate tree be expanded for each initial state to a selected depth, see figure 7.

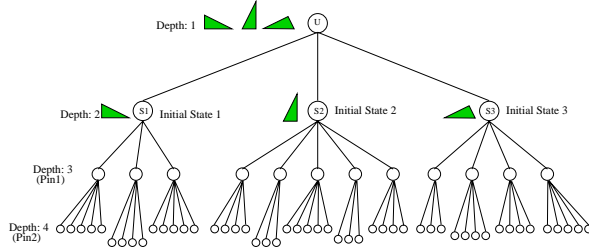


Figure 7 - Tree expansion for each initial state

The principle of combining configuration maps is the same as introduced in [9]. The difference being that the resulting combined map for each tree represents only the transition of one initial state as opposed to all the combined initial states. As we expand the tree, we select pins so that they are guaranteed to be located above or below the possible COMs given the COM position interval, hence avoiding singularities such as metastable states. Metastable refers to states in which the part's motion cannot be predicted and is generally random. Metastable states here would imply that the part could rotate either CW or CCW without certainty. For this same reason we ignore $d=0$ as a contact parameter value.

For a solution we search all the final nodes of the prescribed depth and group them according to the orientation sets. We select nodes indicating final orientation sets that exist in all trees and then backtrack for each one. A solution exists when the same pins throughout each tree yield the same orientation.

III. CONFIGURATION MAPS USING OVERHEAD PINS

A. Static Passive Simulation Results

Overall, we generated 18 configuration maps for each triangular polygon investigated. Each map corresponds to a distinct value of d varying within $[0.1, 0.9]$ and $[-0.1, -0.9]$.

Table 1 illustrates samples of configuration maps corresponding to one triangular polygon. We show for comparison purposes, maps generated using the tip of the COR locus (r_{tip}) only, using the COR calculated via minimum power mechanics as depicted in figure 3 and the experimental results in the 1st, 2nd and 3rd rows respectively. In general, we observed three clear bands within each map.

All plots on the 1st row clearly show wider B_j ranges than those on the remaining two rows. This is due to the increased amount of sliding implied by motion about the r_{tip} . For this reason we cannot use the r_{tip} when modeling the part's motion. In our case, with the stated assumptions, we find the instantaneous COR which dictates the motion of the part and hence we obtain narrower bands as seen in row 2 of table 1 compared to those in row 1, which are desired for planning.

B. Static Passive Experimental Results

Having created configuration maps via simulations, we now compare these to experimental results for validation. For this purpose, we use a simple setup consisting of a roll of Mylar film acting as a conveyor belt and a static passive pin mounted overhead. Figure 8a shows a picture of this setup. Figure 8b on the other hand, shows the static active pin that is used for experimentation with the FT sensor discussed in section V.

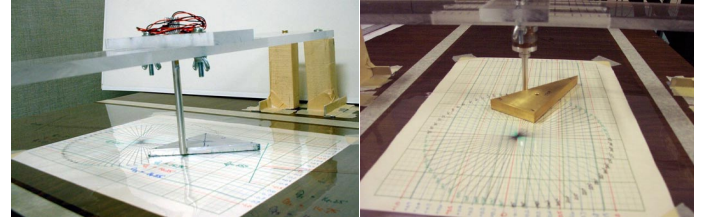


Figure 8 - a) passive pin without sensor and b) active pin with F/T sensor

To create the experimental configuration maps, we carried out three trials for each θ_i and averaged the resulting θ_j to be plotted. Row 3 of table 1 shows the experimental maps for the equivalent values of $d = -0.1$ and 0.3 .

The bands in these experimental maps clearly are narrower than in any of the simulation maps shown. But, comparing rows 2 and 3, we show that the maps created using our calculated CORs provide a good approximation of the part's actual motion; thus, supporting our modeling approach.

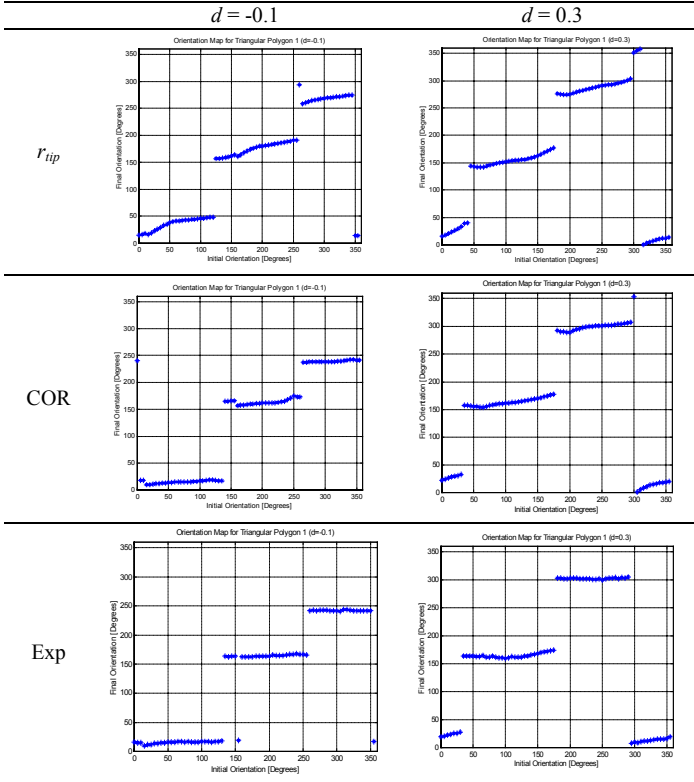
C. Adjusting the Bands' Interval Widths

Comparing the bands' widths between the simulation and experiment configuration maps, rows 2 and 3 respectively, reveal the simulation bands are wider than the experimental counterparts. We attribute the differences to our pressure distribution assumption and numerical errors in the simulation. Thus, we adjust the simulation bands' widths using the B_j intervals' mean (m) and standard deviation (σ) values:

$$B_{j \text{ adjusted}} = m_{B_j} \pm c_{B_j} \quad (7)$$

Thereby removing some of the uncertainty found in the bands' widths. We now compare these adjusted intervals with the experimental intervals. The results showed that the adjusted interval widths are now closer to the experimental results. Also, the adjusted intervals are still larger than the experimental intervals indicating the experimental bands are subsets of the simulation bands. In rare cases we found the opposite. So, since the adjusted intervals match the experimental intervals more closely we justify using the adjusted intervals to seek for a solution.

Table 1 – Configuration maps for given d values. 1st row are maps created using the tip of the COR locus, 2nd row use the estimated instantaneous COR based on minimum power mechanics, and 3rd row are the equivalent maps from experimental trials.



IV. PLANNING RESULTS

We implemented the "fixed-pins" method as illustrated in figures 6 and 7, and figure 2 showed the successful results for all three initial states of a given asymmetrical triangular polygon. Please note that the final orientations of the polygons are contained within the corresponding B_j interval. Thus, they are seen as belonging to a final orientation set rather than a unique orientation. Furthermore, if a part has certain symmetries, a single final orientation band may not be found. Figure 9 illustrates the results for the case where two final orientation bands are found.

The planning results for both asymmetrical (figure 2) and symmetrical (figure 9) polygons were verified experimentally. For each initial state we carried out 10 trials, and all arrived to the same θ_f within $\pm 3^\circ$. A summary of these results is tabulated in table 2.

We are now interested in distinguishing the final orientations obtained in figure 9, and hence finding out the

final result. For this purpose we explore the use of a force/torque sensor to be discussed in the following section.

Table 2 - Pin sequences experimental results

Polygon	Trials	Successes	Failures	Reason
Asymmetrical	10 x 3	29	1	Pin caught vertex
Symmetrical	10 x 3	30	0	n/a

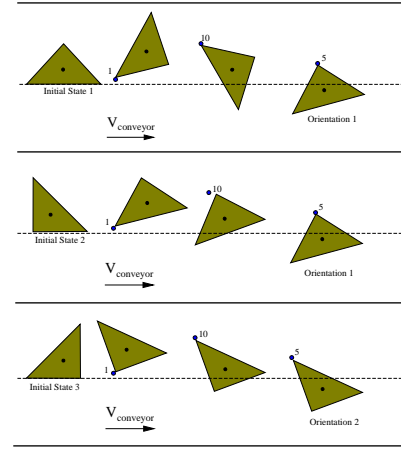


Figure 9 - Pin sequence for symmetric triangular polygon from its three initial states to two final orientations. Pin labels are global labels indicating the chosen pins used to orient all initial states. The sequence must be the same in all cases.

V. INTRODUCING THE FORCE/TORQUE SENSOR

A. Purpose and Approach

We hypothesize that the force/torque (F/T) profiles obtained throughout the period of contact between the part and the pin can provide information on the motion of the part about the pin. We use the sensor where a single final orientation is not found with our search method as in figure 9, but we know the possible final orientations. Hence, in combination with the known planner results we setup the sensor on the first pin of the sequence as in figure 10. Our objective is to distinguish the initial state of the polygon, which in turn will tell us which of the possible final orientations will result; hence, contributing to the orienting process.

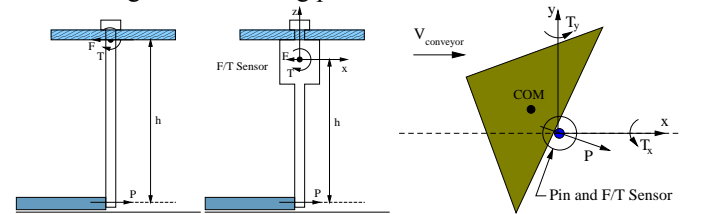


Figure 10 - Pin and F/T sensor setup: side (l) and top (r) view

The expected F/T profiles depend on the geometry and motion of the part as well as its orientation prior to contact with the pin. We emphasize that we are interested in the profiles of the approximate F/T directions rather than their exact directions and magnitudes.

The experimental F/T raw data obtained included a high level of noise. Thus, for the profiles to show visible trends we applied the Moving Averages method to "smooth out" the sensor data.

B. Force/Torque Profiles

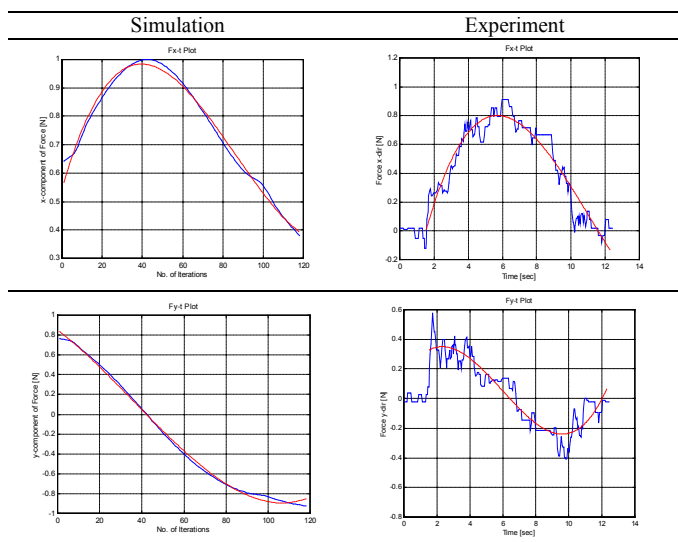
1) Static Active Simulation Results

In theory it is usually not possible to tell the precise direction of the applied force. Whether the part slips with respect to the pin, or it sticks, the force is said to be acting along one of the cone extremes or anywhere within the cone, respectively [6,8]. For the purpose of creating F/T profiles we assume that the force acts perpendicular to the vector between the instantaneous COR and COM. We follow the same simulation procedure as we did in *Section II* where the configuration maps were generated. The results for a simulation trial of $\theta_i = 0^\circ$ and $d = -0.2$ are shown in table 3.

2) Static Active Experimental Results

We plotted the profiles obtained for F_x and F_y using the experimental setup illustrated in figure 8b. Table 3 shows the results for a trial with $\theta_i = 0^\circ$ and $d = -0.2$.

Table 3 - Force profiles and fitted cubic polynomials: simulation (I) and experimental (r)



3) Simulation vs. Experimental F/T Profiles Comparison

Having obtained F/T profiles through both simulations and experiments we now compare their trends empirically. For that purpose, we fit cubic polynomials (dotted curves in table 3) to all the plots using the least-squares method. We decide on cubics for their ability to outline inflection points as well as max/min points.

We calculate the curves' gradients of the F/T components and generate a "sign matrix" $[S]$. This matrix contains the signs of values representing distinct selected regions of the F/T profiles and their gradients' curves. We compare each element against those in a similar matrix for the equivalent simulation trials and set a score for all the matched elements. In this empirical method, we use the scores to decide on which initial state the part is oriented prior to contact with the active pin. Table 4 tabulates the scores for the polygon in figure 9.

Table 4 - Matching scores from Matrix $[S]$ between simulation and experimental trials.

Simulation \ Experiment	Init State 1	Init State 2	Init State 3
Init State 1	35/40	37/40	32/40
Init State 2	35/40	37/40	32/40
Init State 3	28/40	30/40	33/40

C. Planning with F/T Sensor

Comparing the F/T profiles for a given triangular polygon we found that we can distinguish initial states 1 and 2 from 3, but not 1 from 2, as outlined in table 4. This result is due to the initial angle of the edge that contacts the pin with respect to the action line. Using this information along with the planner results yielding two final orientations, we select a pin sequence as in figure 9 such that initial states 1 and 2 yield orientation 1 while initial state 3 yields orientation 2. We can now determine which final orientation will result for any initial state of the given polygon.

VI. CONCLUSION

Although the true motion of a sliding part is unknown, we approximated the instantaneous CORs that dictate the part's motion under the normal pressure distribution assumption.

Using our results of the part's motion, we succeed at orienting a given polygon from a set of unknown initial states to a final orientation using a simple brute-search planner; hence, contributing to the realm of part orienting.

Orienting with pins presents limitations, and in cases a single orientation was not found but the set of initial states was reduced to a smaller set of orientations. Thus we introduced the F/T sensor to aid the orienting process. Finally, we are able to distinguish between the final possible orientations by sensing the possible initial states.

VII. FUTURE WORK

Investigate dynamic pins, that is, pins moving perpendicularly to the direction of the conveyor belt motion. Cases where multiple bands of final orientations exist (passively), we can implement dynamic pins to further orient the part. Preliminary simulation trials have shown that we can take final orientation 1 in figure 9 to final orientation 2; thus, orienting the part to a single final orientation.

REFERENCES

- [1] S. Akella and M. T. Mason. Parts Orienting with Partial Sensor Information. In *IEEE International Conference on Robotics and Automation*, pp 557-564, Leuven, Belgium, 1998.
- [2] S. Akella and M. T. Mason. Parts Orienting with Shape Uncertainty. In *IEEE International Conference on Robotics and Automation*, pp 565-572, Leuven, Belgium, 1998.
- [3] S. Akella, W.H. Huang, K. M. Lynch, and M. T. Mason. Parts Feeding on a Conveyor with a One Joint Robot. *Algorithmica*, 26:313-344, 2000.
- [4] R.P. Berretty, K. Goldberg, M.H. Overmars, and A.F. van der Stappen. Orienting parts by inside-out pulling. In *IEEE International Conference on Robotics and Automation*, pp 1053-1058, Seoul, Korea, 2001.
- [5] S.J. Blind, C.C. McCullough, S. Akella, and J. Ponce. A Reconfigurable Parts Feeder with an Array of Pins. In *IEEE International Journal on Robotics and Automation*, pp 147-153, San Francisco, CA, 2000.
- [6] M. Brokowski, M. Peshkin, and K. Goldberg. Curved Fences for Part Alignment. In *IEEE International Conference on Robotics and Automation*, Atlanta, GA, 1993.
- [7] P.E. Lewis and J.P. Ward, *The Finite Element Method: Principles and Applications*. Addison-Wesley Publishing Co., pp 183-202, 1991.
- [8] M.A. Peshkin and A.C. Sanderson. The Motion of a Pushed, Sliding Workpiece. In *IEEE Journal of Robotics and Automation*, Vol. 4, No. 6, December 1988.

- [9] M.A. Peshkin and A.C. Sanderson. Planning Robotic Manipulation Strategies. In *IEEE Journal of Robotics and Automation*, Vol. 4, No. 5, December 1988.
- [10] M.A. Peshkin and A.C. Sanderson. Minimization of Energy in Quasistatic Manipulation Strategies. In *IEEE Journal of Robotics and Automation*, Vol. 5, No. 1, pp 53-60, 1989.
- [11] S. Rusaw, K. Gupta, S. Payandeh. Determining Polygon Orientation using Model Based Force Interpretation. In *IEEE International Conference on Robotics and Automation*, pp 544-549, Leuven, Belgium, 1998.
- [12] A. Salvarinov and S. Payandeh. Flexible Part Feeder: Manipulating Parts On Conveyer Belt by Active Fence. In *IEEE International Conference on Robotics and Automation*, pp 863-868, Leuven, Belgium, 1998.
- [13] D.E. Whitney. Research Issues in Manufacturing Flexibility – An Invited Review Paper for *ICRA 2000 Symposium on Flexibility*. pp 383-388, San Francisco, CA, 2000.
- [14] R. Zhang and K. Gupta. Automatic Orienting of Polyhedra through Step Devices. In *IEEE International Conference on Robotics and Automation*, pp 550-556, Leuven, Belgium, 1998.
- [15] T. Zhang, G. Smith, R.P. Berretty, M. Overmars, and K. Goldberg. The Toppling Graph: Designing Pin Sequences for Part Feeding. In *IEEE International Journal on Robotics and Automation*, pp 139-146, San Francisco, CA, 2000.